Biochimica et Biophysica Acta 1823 (2012) 2046–2056

Contents lists available at SciVerse ScienceDirect

Biochimica et Biophysica Acta

journal homepage: www.elsevier.com/locate/bbamcr

Structural and biochemical studies of the open state of Lys48-linked diubiquitin ☆

Ming-Yih Lai, Daoning Zhang, Nicole LaRonde-LeBlanc, David Fushman *

Department of Chemistry and Biochemistry, Center for Biomolecular Structure and Organization, University of Maryland, College Park, MD 20742, USA

ARTICLE INFO

Article history:
Received 22 February 2012
Received in revised form 10 April 2012
Accepted 11 April 2012
Available online 16 April 2012

Keywords:
Ubiquitin
Lys48-linked diubiquitin
Polyubiquitin
Ubiquitin-associated domain
Lysine-48 linkage selectivity

ABSTRACT

Ubiquitin (Ub) is a small protein highly conserved among eukaryotes and involved in practically all aspects of eukaryotic cell biology. Polymeric chains assembled from covalently-linked Ub monomers function as molecular signals in the regulation of a host of cellular processes. Our previous studies have shown that the predominant state of Lys48-linked di- and tetra-Ub chains at near-physiological conditions is a closed conformation, in which the Ub–Ub interface is formed by the hydrophobic surface residues of the adjacent Ub units. Because these very residues are involved in (poly)Ub interactions with the majority of Ub-binding proteins, their sequestration at the Ub–Ub interface renders the closed conformation of polyUb binding incompetent. Thus the existence of open conformation(s) and the interdomain motions opening and closing the Ub–Ub interface is critical for the recognition of Lys48-linked polyUb by its receptors. Knowledge of the conformational properties of a polyUb signal is essential for our understanding of its specific recognition by various Ub-receptors. Despite their functional importance, open states of Lys48-linked chains are poorly characterized. Here we report a crystal structure of the open state of Lys48-linked di-Ub. Moreover, using NMR, we examined interactions of the open state of this chain (at pH4.5) with a Lys48-linkage-selective receptor, the UBA2 domain of a shuttle protein hHR23a. Our results show that di-Ub binds UBA2 in the same mode and with comparable affinity as the closed state. Our data suggest a mechanism for polyUb signal recognition, whereby Ub-binding proteins select specific conformations out of the available ensemble of polyUb chain conformations. This article is part of a Special Issue entitled: Ubiquitin Drug Discovery and Diagnostics.

1. Introduction

Ubiquitin (Ub) is a small, 76 a.a. protein [1], highly conserved among eukaryotes and involved in practically all aspects of eukaryotic cell biology [2]. Polymeric chains assembled from covalently-linked Ub monomers function as molecular signals [3] in the regulation of a host of cellular processes, ranging from progression through the cell cycle, to transcriptional activation, antigen processing, and vesicular trafficking of proteins (reviewed e.g. in [2,4–8]). Very remarkably, tagging of a protein with polyubiquitin (polyUb) chains of different linkages commits it to distinct fates in the cell (e.g. [3,7]). Specifically, while K48-linked polyUb chains tag proteins for proteasomal degradation [9,10], K63-linked chains are involved in a variety of non-degradative processes [11–15], and K11-linked chains appear to act both as regulatory and proteolytic signals [8,16,17]. Detailed understanding of the molecular mechanisms underlying specific recognition events is required in order to comprehend the scope of Ub-mediated signaling events and the ability of polyUb to serve as such a versatile and at the same time specific signal. This is critical for designing drugs that target Ub-mediated signaling pathways.

NMR studies have shown that while K63-linked chains adopt an extended conformation in solution [18], the predominant state of K48-linked di- and tetra-Ub chains (Ub_2 and Ub_4, respectively) at near-physiological conditions is a “closed” conformation [19,20], in which the interdomain interface is formed by the surface hydrophobic patches [21,22] (formed by residues L8, I44, and V70) of the adjacent Ub units (Fig. 1). Because these very residues are involved in (poly)Ub's interactions with the majority of the Ub-binding proteins (UBP) [23], their sequestration at the Ub–Ub interface renders the closed conformation of polyUb binding incompetent [24]. Thus the existence of open conformation(s) of polyUb, combined with interdomain motions opening the Ub–Ub interface and making the hydrophobic-patch residues available for binding, is absolutely critical for the recognition of K48-linked polyUb by its receptors. The structure of K48-linked Ub_2 in complex with the Ub-associated (UBA2) domain of the shuttle protein hHR23a serves as an illustration of such an opening [25]. Moreover, the sandwich-like binding mode observed in this complex provides a structural mechanism underlying the K48-linkage selectivity exhibited by UBA2 and several other UBA domains [25,26]. Recent studies have demonstrated that UBPs could vary in their binding preferences toward a particular lysine linkage [26,27]. Unlike the hHR23a UBA2 that forms a sandwich-like complex [25] with K48-linked Ub_2, some UBPs, for example, the UBA domain

☆ This article is part of a Special Issue entitled: Ubiquitin Drug Discovery and Diagnostics.

* Corresponding author at: 1115 Biomolecular Sciences Bldg (#296), Center for Biomolecular Structure and Organization, University of Maryland, College Park, MD 20742-3360, USA. Tel.: +1 301 405 3461; fax: +1 301 314 0386.
E-mail address: fushman@umd.edu (D. Fushman).

0167-4889/$ – see front matter © 2012 Elsevier B.V. All rights reserved.
doi:10.1016/j.bbamcr.2012.04.003

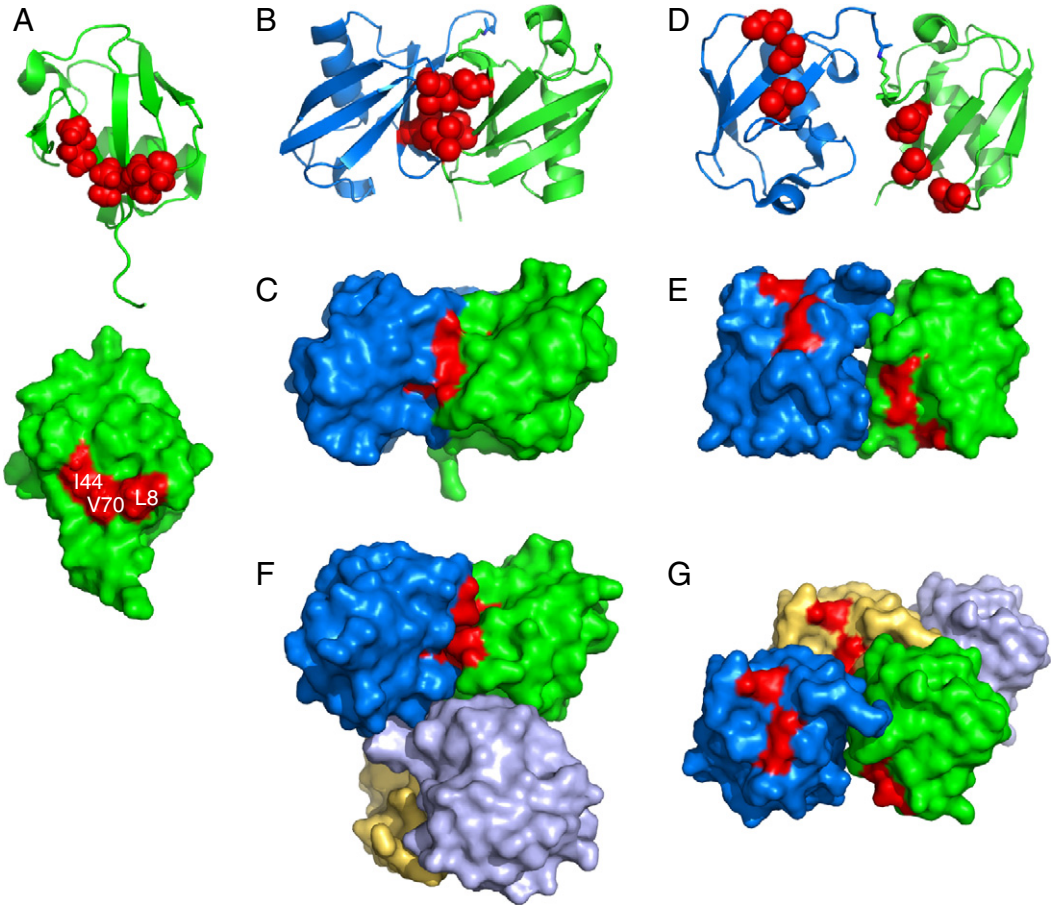

Fig. 1. Crystal structures of Ub and various conformations of K48-linked di- and tetraUb chains. (A) Ribbon and surface representations of Ub structure (PDB ID: 1UBQ). (B and C) Ribbon and surface representations of the closed conformation of Ub_2 (PDB ID: 1AAR). (D and E) Ribbon and surface representations of the open structure of Ub_2 determined here. (F) Surface representation of the closed conformation of Ub_4 (PDB ID: 2O6V). (G) Surface representation of the open conformation of Ub_4 (PDB ID: 1TBE). Following the established terminology for Ub_2 chains, the Ub unit bearing the free C-terminus is referred to as "proximal", while the other Ub, connected to the proximal Ub via isopeptide bond, is called "distal". In the Ub_2 molecules shown here, the distal Ub is colored blue, the proximal Ub is green. In the Ub_4 chains, Ub monomers 1 through 4 (starting with the distal) are colored blue, green, orange, and light blue. In all these drawings, the hydrophobic patch residues L8, I44, and V70 are colored red; their side chains are shown in sphere representation in the ribbon drawings.

of ubiquilin-1 (hPLIC-1) and the UIMs of S5a, bind to both Ub units in the chain independently [28–30]; such binding could require further opening of the chain [29,30]. Therefore, understanding of the structural range of the available conformations of Ub_2 is essential for our understanding of how this and longer chains interact with and are specifically recognized by various Ub-chain receptors in the cell.

It seems reasonable to assume that the conformational ensemble of K48-linked Ub_2 comprises multiple conformations, both open and closed, and in sufficiently fast exchange with each other, such that a ligand molecule could select/bind the proper conformation, thus shifting the conformational equilibrium in the ensemble toward the bound state. Indeed, multiple NMR data from our laboratory revealed that in solution K48-linked Ub_2 exists in fast dynamic equilibrium (on ~10–40 ns time scale) between at least three major conformations [31–33]: the closed one (similar to that observed in the Ub_2 crystals [34–36]), an "open" conformation (previously not observed) with no contact between the hydrophobic patches on Ub units, and an "intermediate" conformation, which resembles the UBA2-bound state [25]. Importantly, the very fact that only a single set of NMR signals is observed in a wide range of conditions (pH from 4.5 up to 8.0) clearly indicates that all these states are in fast exchange on the NMR time scale. Moreover, this equilibrium is pH-dependent: the closed state is predominantly populated at neutral pH (up to 85–90% at pH 6.8) while the open state becomes predominant at acidic conditions (~80% at pH 4.5) [19,32]. Our previous NMR data [19,31,32] provided low-resolution snapshots of open conformations of K48-linked Ub_2, however, only closed conformation(s) of this chain have been observed in crystals [34,36].

A recent study combining X-ray crystallography and NMR [20] showed that pairs of adjacent Ub units in K48-linked Ub_4 adopt a closed conformation that is essentially identical to that of Ub_2. This identifies Ub_2 as the structural element of Ub_4 and longer chains. Interestingly, while both closed and open forms (with and without, respectively, hydrophobic contacts between Ub monomers) of K48-linked Ub_4 were observed in crystals [20,37,38], only closed forms of K48-linked Ub_2 were reported thus far.

Despite the functional importance of the interface opening in K48-linked Ub_2 [24], the open states of this chain are poorly characterized. They have not been directly observed experimentally, and the only available structural information on the open conformations of this chain is in the form of low-resolution models obtained from analyses of ^{15}N relaxation data [19,31–33]. Moreover, binding properties of the open states of K48-linked Ub_2 are not known. Thus, among the outstanding questions to be addressed are: what is the open state of K48-linked Ub_2? Is it binding competent? Is the closed conformation of K48-linked Ub_2 required for the K48-linkage-specific (sandwich-type) binding or can the open conformation of K48-linked Ub_2 result in the same binding mode?

To address some of these questions, here we report a crystal structure of the open state of K48-linked Ub_2. Moreover, using NMR, we examined interactions between the open state of this chain and a K48-selective receptor, the UBA2 domain of hHR23a. We show that,

despite being in an open state at pH 4.5, K48-linked Ub_2 is capable of binding UBPs in the same, sandwich-like mode as at neutral pH (where the chain is predominantly in the closed state). We propose a mechanism for polyUb signal recognition by receptors, whereby Ub-binding proteins select a specific conformation out of the available ensemble of chain conformations.

2. Materials and methods

2.1. Proteins

Ub variants, Ub(K48R) and Ub(D77), were expressed and purified as described [39]. The UBA2 of hHR23a was purified as detailed in [18]. For uniform ^{15}N enrichment, *Escherichia coli* cells were grown in self-inducing medium [40] with $^{15}NH_4Cl$ as the sole source of nitrogen. Unlabeled and segmentally ^{15}N-labeled Ub_2 chains were synthesized through the E1/E2-catalyzed reaction as described elsewhere [19,41]. Ub_2 was separated from unreacted monoUb using a HiLoad 16/60 Superdex 75 prep grade gel filtration column using a 50 mM ammonium acetate, 150 mM NaCl, 5 mM DTT, and 1 mM EDTA pH 4.5 buffer. Pure Ub_2 fractions were collected and verified by SDS-PAGE and NMR.

2.2. Crystallography

The Ub_2 sample used in crystallographic studies was synthesized using the same method as for NMR samples [19,41]. We originally attempted to co-crystallize Ub_2 with the UBA domain of ubiquilin-1 (human homologue of Dsk2), also known as hPLIC-1 [29]. However, the UBA domain was excluded from the crystals during crystallization, leaving us with the crystals of pure Ub_2. Screening was performed using complex protein solution at 20 mg/ml. Crystals were obtained in 100 mM HEPES, pH 7.5, and 20% polyethylene glycol, and cryoprotected in crystallization buffer and 15% ethylene glycol. The X-ray diffraction data were collected at Argonne National Laboratory Advanced Photon Source and processed using HKL2000 [42]. The structure was solved using molecular replacement, with the crystal structure of monoUb (PDB ID: 1UBQ) as the starting model, using MOLREP and refined using REFMAC5 [43–46]. We obtained two Ub molecules per asymmetric unit, which we then confirmed to be linked by an isopeptide bond by observing the difference electron density. Data collection and refinement statistics are shown in Table 1.

2.3. NMR

All NMR experiments were performed using standard pulse sequences on a Bruker 600 MHz spectrometer equipped with a cryoprobe. The sample temperature was 23 °C. ^1H–^{15}N correlation spectra (HSQC and SOFAST) were acquired with the spectral widths (typically) of 7800 Hz and 2100 Hz for the ^1H and ^{15}N dimensions, respectively. A total of 256 t1 increments were collected with 2048 complex points in each. The spectra were processed using XWINNMR or TopSpin (Bruker Biospin). The amide chemical shift perturbations (CSPs) were calculated using the following equation: $\delta = \left(\delta_H{}^2 + \delta_N{}^2/25\right)^{1/2}$, where $\Delta\delta_H$ and $\Delta\delta_H$ are resonance shifts in ^1H and ^{15}N, respectively.

The UBA2 construct alone proved to be unstable at high concentrations at low pH; this made it challenging (or almost impossible) to prepare and keep a high concentration stock of UBA2 at pH4.5 for the titration. Therefore, titrations were performed by starting with 300 µl of 1.15 mM ^{15}N labeled monoUb or Ub_2 at pH4.5 (50 mM NaOAc buffer) and adding 10 µl portions (up to 70 µl total) of the concentrated (5 mM) UBA2 stock at pH6.8 (20 mM phosphate buffer). The change in pH upon the addition of phosphate buffer to the NaOAc buffer was very limited, in the 0.1–0.2 pH unit range, as verified by direct measurements of separate mixtures (mimicking the titration) of the corresponding buffers. We also separately verified that the spectra of Ub before and after the addition of the same amount of phosphate buffer alone (without UBA2) were almost identical. These control NMR experiments ensured that the changes in the spectra in the course of titrations were not from the change in the buffer. For reciprocal titrations, of ^{15}N UBA2 with monoUb or Ub_2, both binding partners were prepared in the same buffer (50 mM NaOAc, pH 4.5).

3. Results

3.1. Crystal structure of an open state of K48-linked Ub_2

We obtained crystals of K48-linked Ub_2 that diffracted at 1.71 Å resolution. The protein crystallized in space group $P2_1$ symmetry, with a single Ub_2 molecule per asymmetric unit. Data collection and refinement statistics are presented in Table 1. The structure of the protein determined at these conditions is shown in Fig. 1D and E. In contrast to the previously described crystal structures of K48–Ub_2 [34,36] (Fig. 1B and C), this structure depicts an "open" conformation of the chain, with no hydrophobic contact between the two Ub monomers. However, this Ub_2 conformation is almost identical to that formed by Ub units 1 and 2 as well as 3 and 4 in another published structure of K48-linked Ub_4 [37] (PDB ID: 1TBE, Fig. 1G): these units superimpose with the backbone RMSD of 0.33 Å (Fig. 2A). Interestingly, the Ub_2 structure obtained here is also almost identical to that formed by the "middle" two units, 2 and 3, in the same Ub_4 structure: the corresponding backbone RMSD is 0.33 Å (Fig. 2B). This symmetry between all pairs of adjacent monomers is perhaps not surprising, since in the absence of specific hydrophobic inter-monomer contacts neither pair is expected to be different from the others. These results clearly indicate general relevance of the open Ub_2 structure observed here to the open conformation(s) of Ub_4 and longer polyUb chains, in that this Ub_2 serves as the building element of the longer chains.

Interestingly, despite being in an open conformation with no hydrophobic contacts between the Ub units, the K48-linked Ub_2 chain obtained here is quite compact. The radius of gyration, $Rg = 16.8$ Å, computed for the structure in Fig. 1D and E only slightly exceeds 16.0 Å computed for the closed conformation (PDB ID: 1AAR, Fig. 1B and C), both being slightly below 17.4 Å measured by small-angle X-ray scattering at pH6.8 [47].

Table 1
X-ray data collection and refinement statistics.

Data collection	Lys48-linked Ub_2
Space group	$P2_1$
Cell dimensions	
a, *b*, *c* (Å)	24.05, 56.50, 46.84
α, β, γ (°)	90, 93.37, 90
Molecules/Asym. unit	1
Wavelength (Å)	0.97927
Resolution (Å)	40–1.71
R_{sym} (last shell)	0.073 (0.18)
$I/\sigma I$	17.3 (5.4)
Completeness (%)	94.4 (72.7)
Redundancy	4.5 (3.7)
Refinement	
Resolution (Å)	18.3–1.71
R_{work}/R_{free} (%)	18.6/23.7
Residues	149
Solvent	Water: 133, glycerol: 2, HEPES: 1
Mean B-factors (Å)^2	21.1
RMS deviations	
Bond lengths (Å)	0.006
Bond angles (°)	1.115
Ramachandran plot	
Favored	100.0%
Additional allowed	0.0%
Disallowed	0.0%

3.2. Crystallographic contacts reveal multiple polar interactions between ubiquitins

Because of the absence of intra-chain hydrophobic-patch contacts between Ub monomers (typically observed in K48-linked Ub_2 in solution and crystals), it is natural to expect that the Ub_2 conformation obtained here is stabilized by inter-chain crystallographic contacts. In fact, the Ub_4 structure 1TBE superimposes ideally on the two neighboring Ub_2 molecules in our crystals (Fig. 2C), the backbone RMSD is 0.34 Å. This indicates that the contacts (both intra- and inter-chain) between Ub units observed in our crystals are the same as in the "open" conformation of Ub_4 (PDB ID: 1TBE) and likely to be present in longer chains. A close inspection of these contacts revealed several electrostatic or polar interactions between neighboring Ub_2 chains; some of them are the same as intra-chain contacts, but some are purely inter-chain interactions.

The largest crystallographic contact interface (~350 $Å^2$) is observed between the proximal Ub of one Ub_2 molecule and the distal Ub of a symmetry related molecule (colored green and orange, respectively, in Fig. 2D–F). This interface is nearly identical to that between the middle Ubs in the Ub_4 chain in 1TBE [37] (Fig. 2C) and is also similar to the (intra-chain) interface between the two Ub units in Ub_2. On one end of the interface, residues R72 and R74 near the C-terminus of the distal Ub of one chain interact via salt-bridges

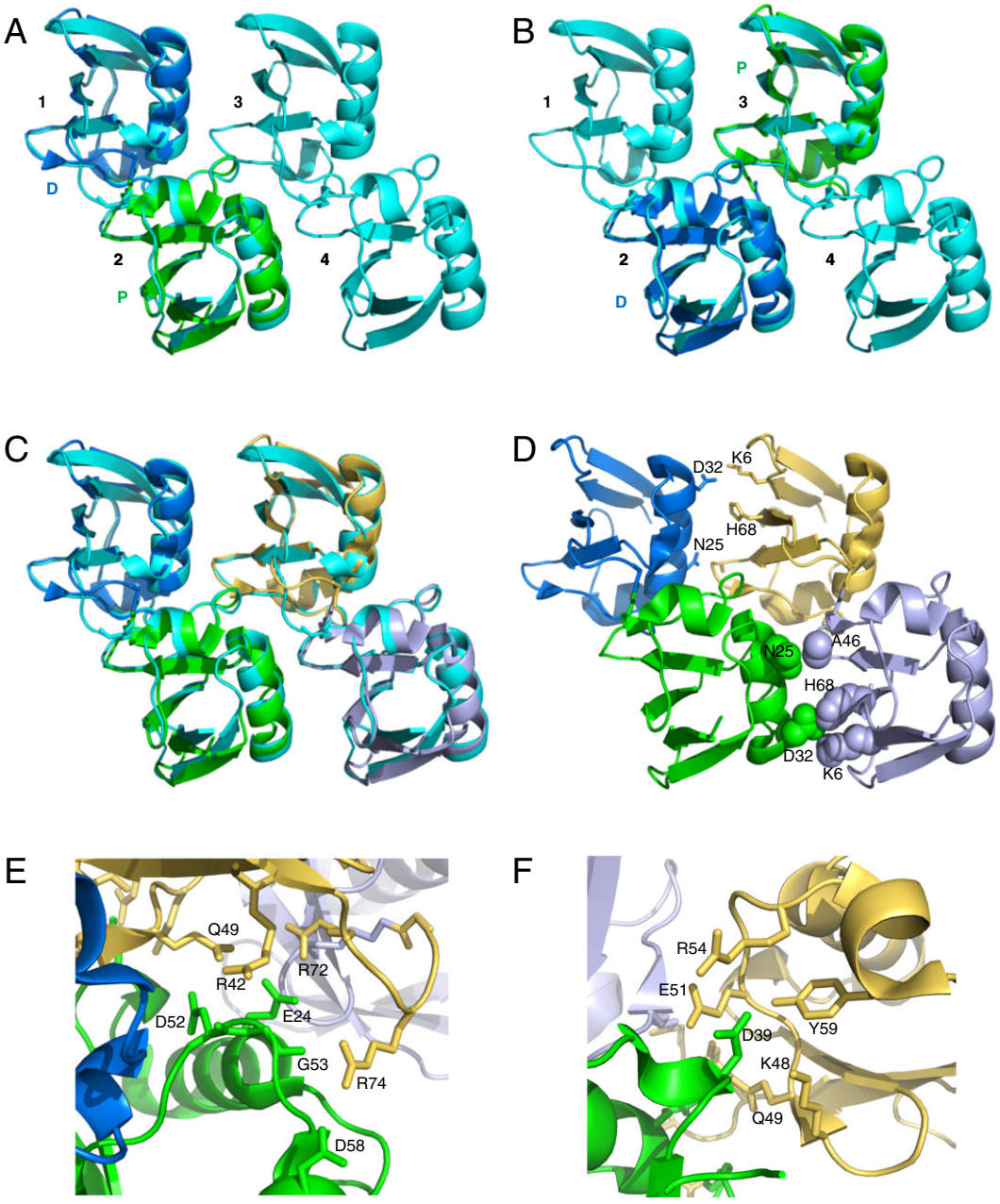

Fig. 2. Comparison with the "open" Ub_4 structure and a close up on the intra- and interchain contacts in Ub_2 crystals. (A and B) Superimposition of the Ub_2 structure obtained here with Ub units 1 and 2 (A) or 2 and 3 (B) of the Ub_4 structure (PDB ID: 1TBE). The Ub_4 chain is colored cyan, while the distal and proximal Ubs in Ub_2 are colored blue and green, respectively. Ub units in Ub_4 are numbered 1 through 4 while the distal and proximal units in Ub_2 are labeled D and P and colored, respectively. (C) Superimposition of the Ub_4 structure (PDB ID: 1TBE) with two neighboring (symmetry related) Ub_2 molecules. The coloring scheme is the same as in A and B except that Ub units in the second Ub_2 molecule are colored orange (distal) and light blue (proximal). The backbone RMSD values are 0.33 Å in A and B and 0.34 Å in C. (D) Inter-chain contacts between similar Ub units of the neighboring Ub_2 molecules: the side chains forming contacts between the proximal Ubs are shown in sphere representation. The same contacts between the two distal Ubs are shown in stick representation. (E and F) A close-up on the crystallographic contacts between the proximal Ub (green) of one Ub_2 molecule and the distal Ub (orange) of its neighboring molecule. Similar contacts are present between the Ub units within the same chain. The coloring of Ub units in the two Ub_2 chains in D and F is the same as in C. Key residues are indicated.

and H-bond with E24 (R72) and D58 and the backbone carbonyl of G53 (R74) of the proximal Ub from the symmetry related chain (Fig. 2E). On the other end, K48, E51, R54 and Y59 of that distal Ub interact with a single residue D39 on that proximal Ub of the other Ub_2 molecule, via salt-bridges with its side chain and H-bonds with the backbone amide nitrogen and carbonyl oxygen (Fig. 2F). In the center of the interface, the only interactions are H-bonds between Q49 from the distal Ub with E24 of the proximal Ub, and between the side chain of R42 (distal Ub) and the backbone carbonyl oxygen of D52 (proximal Ub). There are no hydrophobic contacts in the interface. This interface, rich with polar contacts, is utilized by each Ub_2 molecule to interact with its neighbors to generate the crystal lattice in one direction. In addition, the proximal Ubs of the two neighboring (symmetry related) Ub_2 molecules contact each other via a single H-bond between D32 and K6 as well as van der Waals contacts between N25 and A46 and between D32 and H68 (Fig. 2D, spheres). Similar contacts are present between the distal Ubs of the same two molecules (Fig. 2D, sticks). All these interactions between the neighboring molecules as well as similar (intra-chain) interactions within each Ub_2 molecule contribute the bulk of the crystal packing interaction energy for the open conformation in one plane of the crystal lattice.

Noteworthy, the hydrophobic-patch residues L8, I44, and V70 that mediate interactions at the hydrophobic Ub–Ub interface in the closed conformation of K48-linked Ub_2 are not involved in the crystal packing interactions, except for van der Waals contact between L8 of the distal Ub and I36 of the proximal Ub (and *vice versa*) of a symmetry related molecule above or below the plane of Ub_2 assemblies shown in Fig. 2D. These and additional crystal packing interactions between the Ub_2 planes generate the crystal lattice in the third dimension and are not likely to be physiologically relevant.

3.3. Does the open conformation of K48-linked Ub_2 represent the chain's structure at physiological conditions?

That the open conformation of K48-linked Ub_2 is stabilized by inter-chain contacts in the crystal, which are not expected to be present under physiological conditions, raises the question: *How relevant is the current Ub_2 structure to the chain's conformation in solution?* Clearly, given the transient character of intra-chain Ub–Ub interactions [19] and the conformational flexibility of the Ub–Ub linker [48] (see also Fig. 3G), the effect of packing forces cannot be underestimated. In order to examine the relevance of the open Ub_2 structure at near-physiological conditions, we turned to our solution NMR data for K48-linked Ub_2 [19,48].

Inspection of the open-state crystal structure of K48-linked Ub_2 revealed several non-covalent intra-chain contacts between Ub monomers, which are similar to the inter-chain interactions described above. These include possible H-bonds between the side chains of D52 of the distal Ub and Q49 of the proximal Ub, D39 (distal) Ub and Y59 and R54 (proximal), the isopeptide nitrogen of K48 (proximal) and the backbone carbonyl of D39 (distal), and the side chain of E51 (proximal) and the backbone amide of D39 (distal). Altogether, the distal D39 potentially participates in five interactions at the interface between the two Ub molecules. However, there are essentially no intra-chain hydrophobic interactions. This is in stark contrast with strong and highly specific chemical shift perturbations (CSPs) observed by NMR in the hydrophobic-patch residues at neutral and higher pH (6.8–8.0) and indicative of a hydrophobic contact between Ub units in the chain [19,24]. Furthermore, the interdomain orientation in the open state of Ub_2 (Fig. 1D) is inconsistent with the ^{15}N relaxation data and residual dipolar couplings (RDCs) measured at neutral pH (see [19,48] and also Fig. 3). All these results suggest that the open conformation of K48-linked Ub_2 likely represents a low-populated rather than the predominant state of the chain at neutral pH.

3.4. K48-linked Ub_2 is in open state at acidic conditions

In contrast to neutral pH, no non-covalent intra-chain contacts between Ub monomers were detected in our NMR studies of K48-linked Ub_2 at acidic conditions (pH 4.5) [19]. Thus, it seems reasonable to expect that the crystal structure of an open state of Ub_2 obtained here (Fig. 1D and E) is more relevant to the Ub_2's state at low pH. Indeed, this structure shows no hydrophobic-patch contacts between Ub monomers, and therefore generally agrees with our NMR data at low pH. The natural question then is, *whether this structure represents the predominant conformation of K48-linked Ub_2 in solution at acidic conditions.* A detailed comparison with our ^{15}N relaxation data and $^{1}H–^{15}N$ RDCs measured at pH 4.5 indicates that it is not the case. For example, while the structure of each Ub unit fits the ^{15}N relaxation data quite well (the correlation coefficients are 0.94 for the distal ($Q = 0.24$) and 0.95 ($Q = 0.21$) for the proximal Ub), fitting the same data for the two Ub units *together* reduced the correlation dramatically ($r = 0.63$, $Q = 0.59$) (Fig. 3). This indicates that the open Ub_2 structure observed in the crystals—while being a valid snapshot of a particular conformation of this chain—does not represent the full conformational ensemble of Ub_2. Furthermore, the interdomain orientation in the open structure (Fig. 1D) differs from that derived from ^{15}N relaxation measurements at acidic pH (see [19,48]), thus suggesting that this structure does not represent the average solution conformation of Ub_2 at these conditions. The analysis of $^{1}H–^{15}N$ RDC data yields similar results (not shown). Note that of all residues involved in the polar intra-chain contacts in the open structure (see above), only Y59, K48, and Q49 (all in the proximal Ub) show noticeable shifts in the amide NMR signals compared to free Ub at pH 4.5 (see [19]); the perturbations in the latter two residues, however, could reflect K48's involvement in the isopeptide bond.

The rotational diffusion tensors extracted from the ^{15}N relaxation data (at pH 4.5) for each Ub unit in Ub_2 (Fig. 3) show a two-fold slower tumbling compared to monomeric Ub ($\tau_c \sim 8.4$ ns versus 4.3 ns) and the degree of rotational anisotropy (~1.5), consistent with the two Ubs tumbling as a single moiety (to a first approximation). However, the backbone order parameters extracted from the ^{15}N relaxation data at pH 4.5 (Fig. 3G) and at pH 6.8 [48] clearly indicate that the C-terminus of the distal Ub is quite flexible ($S^2 \sim 0.4$), albeit less flexible than the free C-terminus of the proximal Ub. These data point to some degree of interdomain dynamics that inevitably results in conformational flexibility of Ub_2 in solution.

3.5. UBA2 binding to monoUb at acidic conditions

As shown in [25], the extended hydrophobic pocket and the ability of K48-linked Ub_2 to bind receptors in a sandwich-like fashion are the underlying structural determinants for the K48-linkage selectivity observed in the UBA domains. Note that the Ub_2–UBA2 complex, with the sandwich-like arrangement of the two Ub units around UBA2, was observed at neutral pH, where the closed form of Ub_2 is predominant. K48-linked Ub_2 can also exist in an open, albeit less populated, state at these conditions, as evident from the fact that the crystal structure obtained in this study was observed in crystals grown at pH 7.5. That the hydrophobic patches of both Ubs are exposed and available for ligand binding in the open state of Ub_2 raises several important questions, namely, (i) if the Ub_2 chain in this state is still capable of binding UBA2, and (ii) if it binds UBA2 in a similar fashion as for the predominantly closed state or perhaps as for the open, K63-linked Ub_2 (in other words, will the open state of Ub_2 close to form a sandwich-like complex with UBA2 or will it remain open in the UBA2 bound state?). To address these questions, we needed the environment that would allow us to "lock" K48-linked Ub_2 in an open state. As mentioned above, our NMR data clearly show that at pH 4.5 the preferred state of K48-linked Ub_2 is an open state, with no non-covalent intra-chain contacts between Ub monomers. Therefore

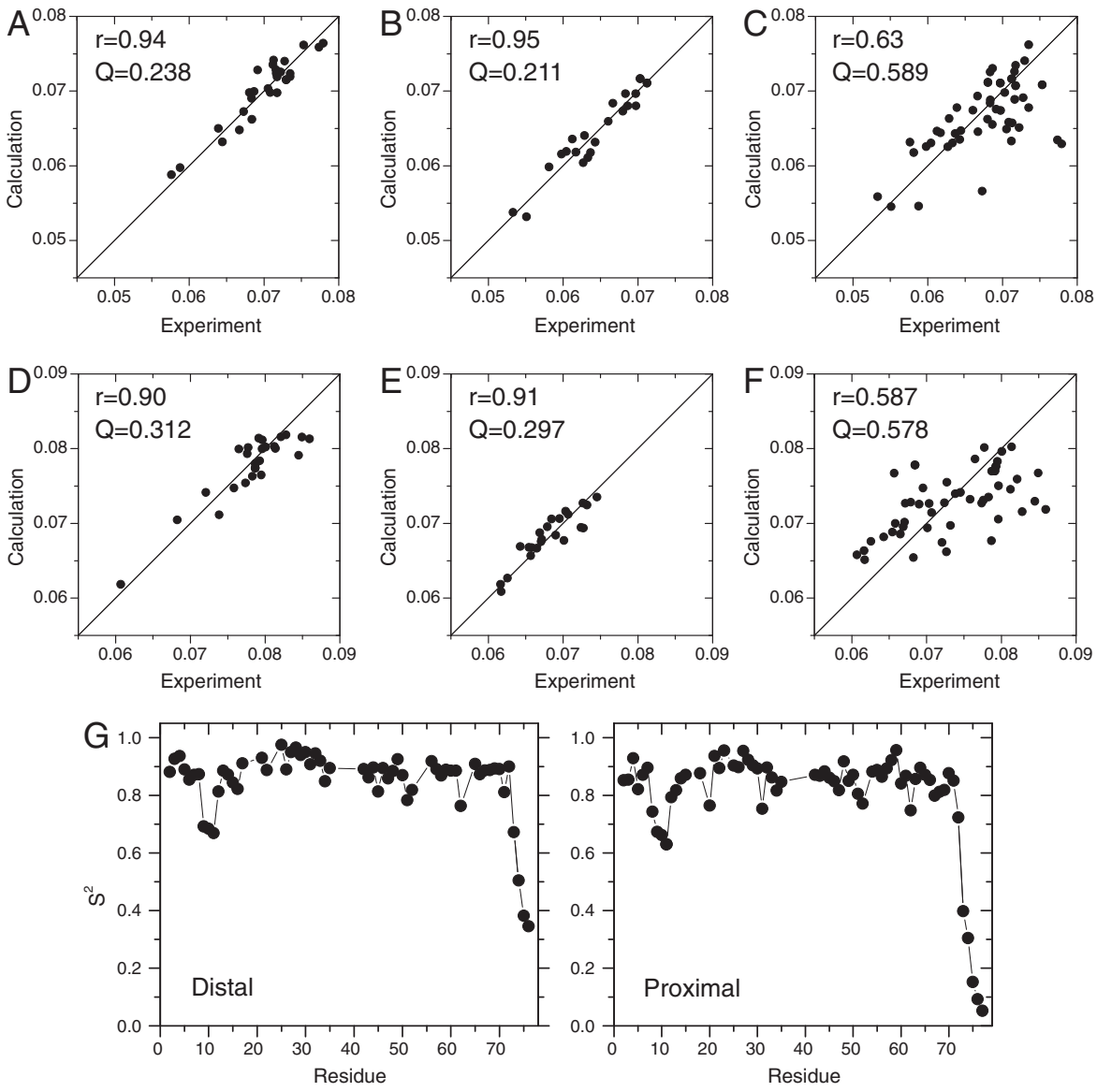

Fig. 3. NMR analysis of the conformation and dynamics of K48-linked Ub_2 in solution. (A–D) Comparison of the "open" Ub_2 structure with ^{15}N relaxation data measured at pH 4.5 (A–C) and pH 6.8 (D–F). Shown is the agreement between the experimental and back-calculated ratio of relaxation rates [48], $\rho = \left(2\frac{R_2}{R_1} - 1\right)^{-1}$, for (A and D) the distal Ub, (B and E) the proximal Ub, and (C and F) both domains taken together. Values of the Pearson's correlation coefficient (r) and the fit-quality factor (Q) are indicated. The analysis of ^{15}N relaxation data for the distal Ub (panel A) provided the overall rotational correlation time for Ub_2 of $\tau_c = 8.22 \pm 0.23$ ns and the anisotropy of the rotational diffusion tensor $\eta = 1.50 \pm 0.09$. The corresponding parameters extracted from the proximal Ub data (B) are $\tau_c = 8.49 \pm 0.29$ ns, $\eta = 1.33 \pm 0.10$. (G) Backbone order parameters as a function of residue number for the distal (left) and proximal (right) Ubs in Ub_2.

we chose these conditions to examine the ligand-binding properties of the open state of K48-linked Ub_2.

Prior to characterizing the UBA2's binding to Ub_2, we examined its binding to monoUb. The rationale for these studies was twofold. First, no studies of Ub binding to UBA2 or other Ub-receptor were performed at acidic pH so far. Second, these data serve as a control, if we want to understand whether binding to Ub_2 is different from binding to monoUb or, in other words, whether UBA2 binds to K48-linked Ub_2 *differently* from independent binding to each individual Ub monomer in an open chain. Note in this regard that UBA2's binding to K63-linked Ub_2 (which is in open conformation) is essentially the same as binding to monoUb [18], i.e. the two Ub units in that chain behave as independent UBA2-binding sites.

These binding studies were performed by "looking" at both interacting partners using NMR spectroscopy. Specifically, ^{15}N labeled Ub was titrated with unlabeled UBA2, and *vice versa*, and the binding was monitored through changes in the ^{1}H–^{15}N HSQC spectra recorded at each titration step (see e.g. [25,29]). The results are summarized in Fig. 4. Overall, the mode of Ub–UBA2 binding is similar to that at neutral pH. The binding interface on Ub involves the hydrophobic-patch surface centered at residues L8, I44, V70. On the UBA2 side, the spectral perturbations observed involve the loop connecting helices α1 and α2 (residues 330–332) and the N-terminus of helix α3 (residues 348–352)—the "canonical" Ub-binding surface on the UBAs [18,25,29,49,50]. Also the relatively weak affinity ($K_d \sim 215 \pm 35$ μM) is characteristic for the UBA2 binding to monomeric Ub [18,49]. All these data indicate that the monoUb–UBA2 interaction at pH 4.5 is similar to that at neutral pH, thus setting the stage for studies of UBA2 binding to Ub_2.

3.6. Open state(s) of K48-linked Ub_2 maintain K48-specific ligand binding properties

We then performed similar binding studies (at pH 4.5) for K48-linked Ub_2. In order to distinguish between UBA2 binding to the distal

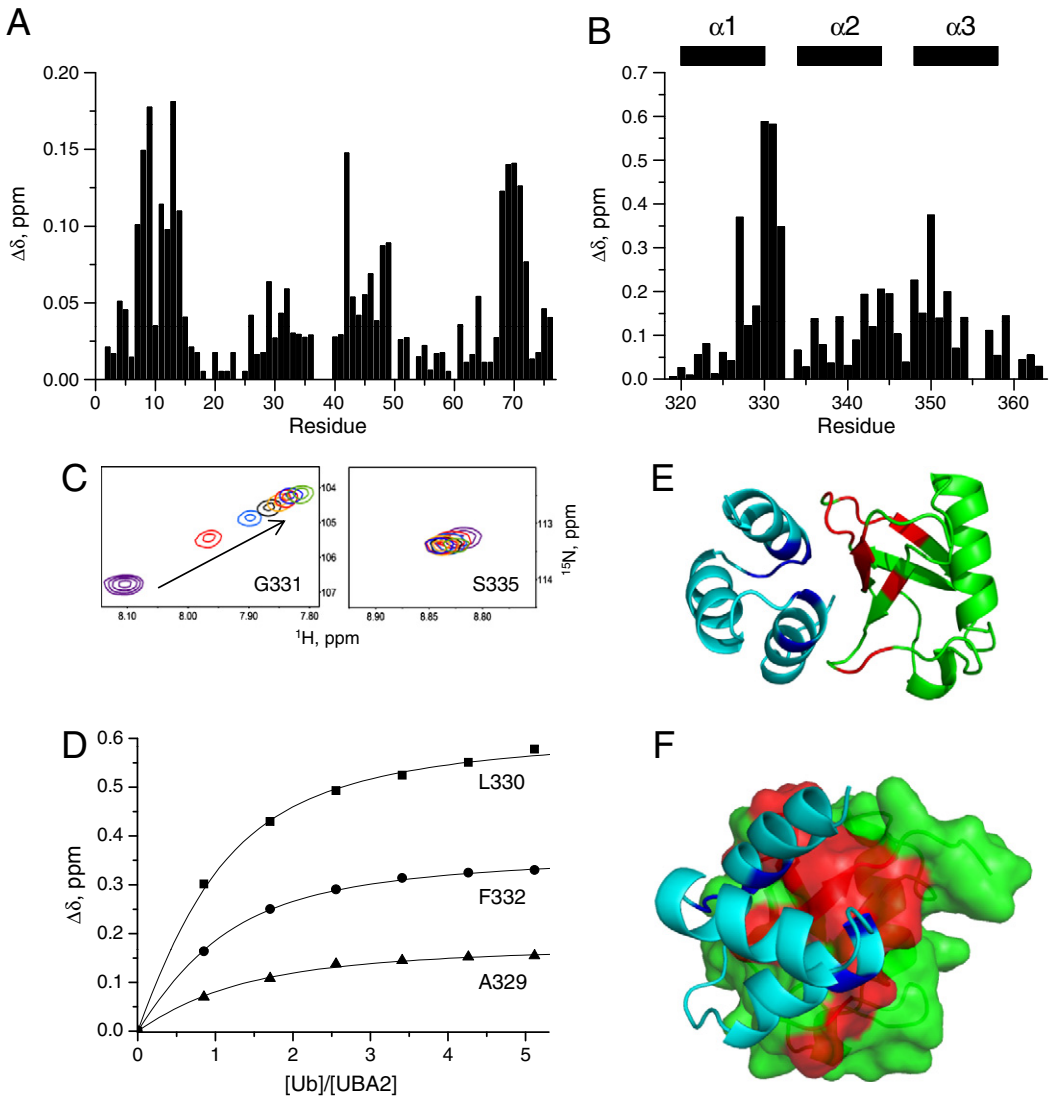

Fig. 4. NMR studies of the interaction between Ub and hHR23a UBA2 at pH 4.5. (A) Chemical shift perturbations in the individual amides in Ub caused by UBA2 binding. (B) Chemical shift perturbations in the individual amides in UBA2 caused by Ub binding. Data in both (A) and (B) correspond to the endpoints in titration. The horizontal bars on top of the plot in (B) indicate the location of UBA2's α-helices. (C) Overlay of ^{1}H–^{15}N HSQC spectra of ^{15}N-labeled UBA2 at several titration points with unlabeled Ub; shown are regions corresponding to signals of G331 and S335. (D) Representative titration curves (symbols) and their fit to a 1:1 binding model (curves) for selected amides in ^{15}N-labeled UBA2 upon addition of Ub. The K_d value averaged over 11 residues was 215 ± 35 μM. (E and F) Map of the perturbations in Ub and UBA2 observed in this study (pH 4.5) on the structure of the Ub–UBA2 complex obtained at neutral conditions [25,50]. UBA2 is shown as a ribbon (cyan), while Ub is colored green and shown as a ribbon in E and as a surface in F; the perturbed residues are colored red (Ub) and blue (UBA2).

and the proximal Ub units, we used two Ub_2 constructs which are identical chemically but differ in which Ub unit is ^{15}N enriched (hence served as a reporter in our NMR measurements). In order to map the binding surface on hHR23a UBA2, uniformly ^{15}N labeled protein was titrated with unlabeled Ub_2.

The results of our studies are summarized in Fig. 5. In contrast to UBA2 binding to monoUb (Fig. 4) (and to K63-linked Ub_2 [18]), the two Ub units behaved differently upon their titration with the UBA2. Here the proximal Ub exhibited spectral perturbations right away, already at the first titration steps, and the CSPs saturated at the UBA2/Ub_2 molar ratio of approximately 1, suggesting strong UBA2 binding to this unit, with 1:1 stoichiometry. Fitting the titration curves (Fig. 5F) yielded K_d values in the micromolar range (1.4 ± 1.0 μM), which is a dramatic increase in the binding affinity compared to monoUb. This is consistent with similar observations at neutral pH [25,27] and indicates that hHR23a UBA2 retains its selectivity for K48-linkage also at acidic conditions. By contrast, the NMR spectra of the distal Ub showed very little changes at the beginning of titration. The perturbations here continued to slowly increase upon further addition of UBA2 but have not reached saturation at the endpoint of titration ([UBA2]:[Ub_2] = 2.7), indicating a significantly weaker binding compared to the proximal Ub (Fig. 5F). Such differential behavior of the two Ub units in K48-linked Ub_2 in their interaction with hHR23a UBA2 is fully consistent with that observed at neutral conditions [25]. Furthermore, in full agreement with the mode of binding (previously observed at pH 6.8 [25]) in which UBA2 first binds to the proximal Ub and the Ub–Ub linkage, the perturbation of the isopeptide signal saturated at the same titration steps as the backbone amides in the proximal Ub, and several residues in the distal Ub (T7, V70, and later I44 and the C-terminus) showed strong signal attenuations early in the titration.

Using NMR, we also monitored binding "reported" by the UBA2 domain. The spectral perturbations observed in ^{15}N-labeled UBA2 upon binding to Ub_2 suggest that additional UBA2 residues are affected compared to monoUb binding. Importantly, we detected strong perturbations in helix α2 located on the "backside" of UBA2 (Fig. 5G) which are the hallmark of the sandwich-type binding at neutral pH [25]. It is noteworthy that many UBA2 signals were

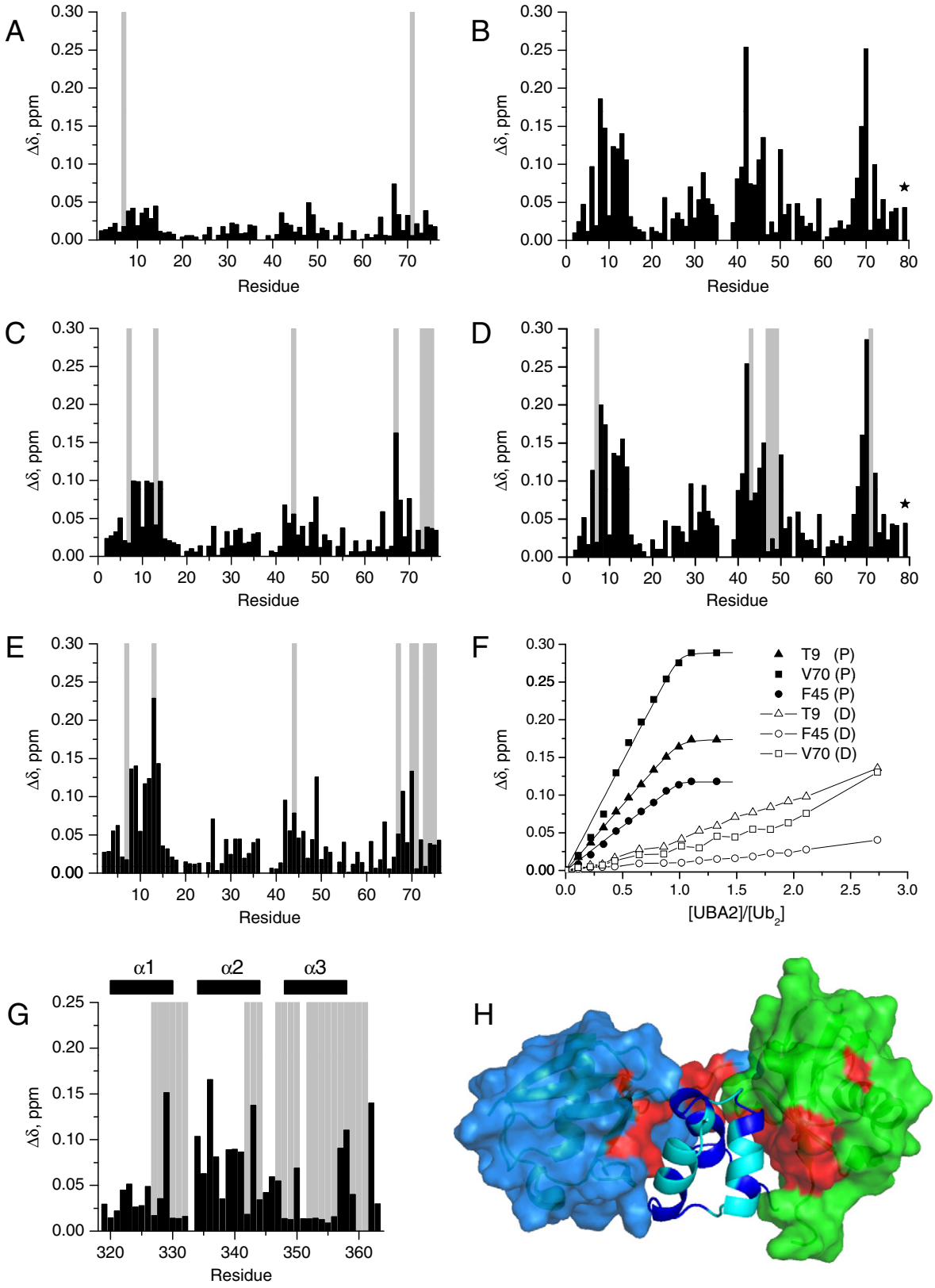

Fig. 5. NMR analysis of hHR23a UBA2 binding to K48-linked Ub_2 at pH 4.5. (A–E) Spectral perturbations in backbone amides in the distal (left column) and the proximal (right column) Ubs at similar points in titration: the UBA2/Ub_2 molar ratios are 1.0 (A, B), 1.25 (D), 2.0 (C), and 2.7 (E). The CSP in the amide group of the isopeptide bond is also shown, as residue 79 (in B and D) and marked with a star. Gray vertical bars indicate residues showing strong signal attenuation in the course of titration, indicative of intermediate or slow exchange. (F) Representative binding curves for the proximal Ub (solid symbols) and the distal Ub (open symbols) upon UBA2 titration. The lines for the proximal-Ub data represent the results of fit to a 1:1 binding model (assuming that binding to the distal Ub is negligible at these steps in titration), while the lines for the distal data merely connect the data points. The dissociation constant for the proximal Ub obtained from this fit was $K_d = 1.4 \pm 1.0$ μM (averaged over 11 residues). (G) Spectral perturbations in UBA2 induced by binding to Ub_2, at the Ub_2/UBA2 molar ratio of 0.2. Most of the UBA2 signals were broadened beyond detection at later steps in the titration as a result of slow exchange. (H) Map of the spectral perturbations observed in Ub_2 in this study (pH 4.5) on the Ub_2–UBA2 structure obtained at neutral pH [25]. The distal Ub is colored blue, the proximal is green, and residues showing significant CSPs and/or signal attenuations are colored red.

significantly broadened, often beyond detection. Such behavior is indicative of an intermediate or slow exchange on the NMR time scale, reflecting slow off-rates, hence stronger binding. The detection of residue-specific CSPs and signal attenuations allowed us to map out the Ub_2-binding surface, which now includes the "backside" of UBA2, and is consistent with the sandwich-like mode observed at neutral pH.

In order to assess the stoichiometry of the binding interactions, we measured the rates of spin-relaxation of ^1H and ^{15}N nuclei, which reflect the rates of the overall tumbling of a molecule, and therefore are a sensitive indicator of the size of the complex. The transverse relaxation time of amide protons (^1H T_2) showed a decrease from ~50 ms for free monoUb to 28.5 ms for the Ub–UBA2 complex, generally consistent with the 1:1 stoichiometry of binding. Upon titration with UBA2, the ^1H T_2 decreased from ~25 ms for free Ub_2 to 16.8 ms for UBA2–Ub_2 complex at the 1.1:1 molar ratio, suggesting that at these conditions approximately one UBA2 molecule is bound to Ub_2. Adding more UBA2 to Ub_2 resulted in a further increase of the size of the complex, as evident from the increase in the ^{15}N longitudinal relaxation time (T_1) from 699 ± 38 ms for the free Ub_2 to $T_1 = 961 \pm 49$ ms measured for the distal Ub at the endpoint of titration ([UBA2]:[Ub_2] = 2.7). The latter value corresponds to the molecular weight of approximately 26 ± 2 kDa [25], which falls between 23.2 kDa and 29.2 kDa expected for 1:1 and 2:1 UBA2:Ub_2 complexes, respectively. This is consistent with the onset of binding of a second UBA2 molecule, presumably to the distal Ub (Fig. 5), as has also been observed at neutral pH [25].

All these results indicate that despite being in the open state, K48-linked Ub_2 is perfectly capable of binding its receptors (e.g., hHR23a UBA2) in the same (sandwich-like) mode as for the closed state and with comparable affinities.

4. Discussion

Unlike other post-translational modifications of proteins, such as phosphorylation, acetylation, methylation, etc., the covalent attachment of ubiquitin or a polyubiquitin chain results in a vast range of potential signals, thus providing a versatile signaling mechanism for various cellular events. Using a protein as the signaling unit allows selection of binding partners (proteins or protein domains) capable of forming large and specific interaction surfaces with Ub. Having multiple Ubs in one chain not only serves the purpose of enhancing the "strength" of the Ub-signal but also—and perhaps most importantly—results in numerous spatial arrangements of the Ub-signals (hence potentially a new signal) by virtue of the various ways how Ub monomers can be linked to each other. Ub interacts with the majority of its binding partners through a rather shallow hydrophobic patch on its surface, surrounded by several basic residues, whereas the acidic side chains are mostly located on the opposite face of the protein. The underlying structure–function hypothesis is that the chain linkage (and possibly chain length) defines the ensemble of structures/conformations that a particular chain can adopt [3,23], wherein each conformation displays a unique three-dimensional arrangement of the hydrophobic patches and/or other ligand-binding features. This, in turn, defines the chain's ability to interact with specific receptors (which often contain several Ub-binding domains) in a linkage-dependent manner (e.g. [25,26,30,51–53]). This mechanism of linkage specificity hinges on conformational flexibility of polyUb, which is due in part to Ub's flexible C-terminus (residues 72–76) and in part to the weak interactions (hydrophobic or polar) between Ub units in the chain. The dynamic nature of polyUb is evident, for example, from the various conformations in which K48-linked chains had been crystallized [20,34,37,38], and the open structure of K48-linked Ub_2 observed in this study provides an additional evidence for this.

Ironically, the Ub_2 structure obtained in crystals grown at pH 7.5 (current study) represents an open form that has not been observed at this pH in solution, but instead, is predominant at low pH (pH 4.5) [19]. Likewise, the Ub_2 structure obtained in crystals grown at pH 4.5 (PDB ID: 1AAR [34]) is in stark contrast with the NMR data at that pH, but instead agrees nicely with the chain's conformation in solution at neutral pH [19]. These results (i) serve as evidence that both open and closed conformations co-exist at both pH conditions, and (ii) point to intrinsic flexibility of polyUb chains and the critical role that crystal packing forces could play in shaping their structures observed in crystals.

Based on our analysis of crystal packing for the open structures of K48-linked Ub_2 and Ub_4, it is clear that the open form of Ub_2 is present in solution and is selected during crystal formation. Also evident is that the open form of Ub_2 is the basic structural unit of the Ub_4 chain in 1TBE (Fig. 1G, 2A–C), while the closed form of Ub_2 is the basic structural unit for Ub_4 in 2O6V (Fig. 1F) as well as in an alternative form in 1F9J [38]. Although both Ub_2 and Ub_4 exist in open forms, it is likely that the specific structure observed here (and in 1TBE) is a result of crystal packing forces. Indeed, the crystal packing interfaces for the open form are largely electrostatic, and all contacts identified here are considered unlikely to be physiologically relevant by interface and assembly analysis using PDBe PISA [54]. Our solution NMR data indicate that at physiological conditions both Ub_2 and Ub_4 prefer the closed form (stabilized primarily by hydrophobic Ub–Ub contacts) [19], whereas it is an open form of Ub_2 (and likely of Ub_4) that is the predominant one at low pH (pH 4.5). The specific 3-D structure observed in our crystals (and stabilized by the packing forces) likely represents one of several (if not more) conformations of K48-linked Ub_2 in solution; based on NMR data, the majority of these chains are in an open state at acidic conditions.

As our biochemical data demonstrate, the open state of Ub_2 is an active, binding-competent form, in which the hydrophobic patches on Ub units in the chain are exposed and readily available for interactions with UBPs. Even in the context of Ub_4 and longer chains, and even if there is interaction via the polar interfaces seen in the open-form crystals, the hydrophobic patches on Ub units in these chains remain solvent/ligand accessible (Fig. 1E and G). Therefore it is likely that the open conformation observed in crystals does exist in solution for some fraction of the time, and could be selected out by specific interactions with a Ub-interacting molecule.

Our analysis of the binding properties of K48-linked Ub_2 under acidic conditions, when the chain is predominantly open, demonstrates that, despite being in an open conformation, the Ub_2 retains its ability to interact with ligands (specifically UBA2) through a 3-D conformation that involves a close arrangement of the Ub units resulting in a sandwich-like complex, similar to that observed at neutral pH, when the Ub_2 chain is predominantly closed. Moreover, the fact that UBA2 binding to this chain is much tighter than to monomeric Ub and involves interactions with the linker region, indicates that UBA2 also retains its selectivity for K48-linkage at low pH. Thus, regardless of its predominantly populated conformational state, K48-linked Ub_2 is capable of forming a tight, sandwich-like complex with a K48-linkage selective receptor, like UBA2 of hHR23a.

We propose that hHR23a UBA2 (and possibly other receptors) bind Ub_2 and longer chains through a mechanism in which out of the ensemble of all available chain conformations that co-exist in solution, UBA2 selects those that are "predisposed" to form a tightly-bound sandwich-like complex. This picture agrees with our current and previous observations that K48-linked Ub_2 exists in multiple conformations which are in fast exchange with each other, and at least some of them (populated at about 15–20% at both neutral and acidic pH) resemble those in the Ub_2–UBA2 complex (see [31,32]). Following UBA2 binding to those weakly-populated states of the chain, fast equilibrium exchange within the conformational ensemble of unbound Ub_2 molecules would re-populate the "predisposed" conformations,

thus facilitating further UBA2 binding. Weak non-covalent intra-chain contacts between Ub units (observed here, and also in [19]) together with the significant flexibility of the covalent Ub–Ub linker (see [48]) are responsible for the intrinsic flexibility of polyUb, and therefore are the key elements for such mechanism. An alternative explanation, involving an induced-fit mechanism whereby UBA2 would cause open Ub_2 to partially close and closed Ub_2 to open, resulting in both cases in a sandwich-like complex with UBA2, seems less likely.

Many Ub-receptor proteins contain several Ub-binding domains, most of which recognize the hydrophobic patch on Ub. The specificity for chains of particular linkages likely lies in the ability of those domains to act in tandem by recognizing and binding to a specific arrangement of the hydrophobic patches (or other interaction surfaces) of several Ub units in the chain. Designing compounds specifically targeting Ub-signaling pathways could, therefore, require not only detailed atomic-resolution information on a ligand's interactions with an isolated Ub monomer, but also knowledge of the structural properties and the extent of conformational variability for a specific type of polyUb chain. For example, one might expect that stabilization of the closed conformation of polyUb could universally interfere with UBP's binding to it. All this emphasizes the necessity and importance of understanding and treating polyUb chains as structurally dynamic rather than static signals.

5. Conclusions

Here we report a crystal structure of the open conformation of Lys48-linked Ub_2. The comparison with existing crystal structures of Lys48-linked polyUb chains shows that the new structure is essentially identical to that formed by the adjacent Ub units in the open conformation of Ub_4. Because the NMR data indicate that there are no obvious physical forces that would hold the two Ub units in this particular conformation in solution, it is natural to anticipate that the Ub_2 structure reported here likely represents a snapshot (consistent with crystal packing forces) of one of many open conformations of this chain. Nevertheless, this finding is important because it demonstrates that (i) K48-linked Ub_2 can adopt an open conformation in crystals, and (ii) K48-linked Ub_2 does exist in an open form in solution even at crystallization conditions where the closed Ub_2 conformation is predominant. Furthermore, our results provide structural insights (important for modeling of polyUb–receptor interactions) into (iii) a possible conformation of Ub_2 in the open state and (iv) the interactions and the conformational space available to Lys48-linked polyUb. Last but not least, this structure lends further support to the notion that Ub_2 is the minimal structural unit for longer polyUb chains.

Furthermore, our NMR binding studies at acidic conditions, when the open state of Lys48-linked Ub_2 is the predominant one, show that this chain is capable of binding UBPs in the same mode as observed for the closed conformation of the chain, predominantly populated at neutral pH. The finding that Ub_2 has similar ligand-binding properties regardless of the conformational state of the chain that is mostly populated at specific buffer conditions is generally consistent with a conformational selection mechanism for ligand recognition of and binding to polyUb chains.

Acknowledgements

This work is supported by the National Institutes of Health grants GM065334 and GM095755 to D.F. This work is based upon research conducted at the Advanced Photon Source on the Northeastern Collaborative Access Team beamlines, which are supported by award RR-15301 from the National Center for Research Resources at the National Institutes of Health. Use of the Advanced Photon Source is supported by the U.S. Department of Energy, Office of Basic Energy Sciences, under contract no. DE-AC02-06CH11357. The atom coordinates have been deposited with the Protein Data Bank, PDB ID: 3NS8.

The results described here were presented at the 2011 Ubiquitin Drug Discovery and Diagnostics Conference (UDDD 2011). While this manuscript was in preparation, a paper appeared in press [55] describing a similar crystal structure of the open state of Ub_2.

References

[1] G. Goldstein, M. Scheid, U. Hammerling, D.H. Schlesinger, H.D. Niall, E.A. Boyse, Isolation of a polypeptide that has lymphocyte-differentiating properties and is probably represented universally in living cells, Proc. Natl. Acad. Sci. U. S. A. 72 (1975) 11–15.
[2] A. Hershko, A. Ciechanover, The ubiquitin system, Annu. Rev. Biochem. 67 (1998) 425–480.
[3] C.M. Pickart, D. Fushman, Polyubiquitin chains: polymeric protein signals, Curr. Opin. Chem. Biol. 8 (2004) 610–616.
[4] M. Muratani, W.P. Tansey, How the ubiquitin–proteasome system controls transcription, Nat. Rev. Mol. Cell Biol. 4 (2003) 192–201.
[5] R.C. Aguilar, B. Wendland, Ubiquitin: not just for proteasomes anymore, Curr. Opin. Cell Biol. 15 (2003) 184–190.
[6] M.A. Osley, H2B ubiquitylation: the end is in sight, Biochim. Biophys. Acta 1677 (2004) 74–78.
[7] F. Ikeda, I. Dikic, Atypical ubiquitin chains: new molecular signals. 'Protein Modifications: Beyond the Usual Suspects' review series, EMBO Rep. 9 (2008) 536–542.
[8] K. Wickliffe, A. Williamson, L. Jin, M. Rape, The multiple layers of ubiquitin-dependent cell cycle control, Chem. Rev. 109 (2009) 1537–1548.
[9] V. Chau, J.W. Tobias, A. Bachmair, D. Marriott, D.J. Ecker, D.K. Gonda, A. Varshavsky, A multiubiquitin chain is confined to specific lysine in a targeted short-lived protein, Science 243 (1989) 1576–1583.
[10] M.H. Glickman, A. Ciechanover, The ubiquitin–proteasome proteolytic pathway: destruction for the sake of construction, Physiol. Rev. 82 (2002) 373–428.
[11] J. Spence, S. Sadis, A. Haas, D. Finley, A ubiquitin mutant with specific defects in DNA repair and multiubiquitination, Mol. Cell. Biol. 15 (1995) 1265–1273.
[12] C. Hoege, B. Pfander, G.L. Moldovan, G. Pyrowolakis, S. Jentsch, RAD6-dependent DNA repair is linked to modification of PCNA by ubiquitin and SUMO, Nature 419 (2002) 135–141.
[13] L. Sun, Z.J. Chen, The novel functions of ubiquitination in signaling, Curr. Opin. Cell Biol. 16 (2004) 119–126.
[14] L. Hicke, R. Dunn, Regulation of membrane protein transport by ubiquitin and ubiquitin-binding proteins, Annu. Rev. Cell Dev. Biol. 19 (2003) 141–172.
[15] J. Spence, R.R. Gali, G. Dittmar, F. Sherman, M. Karin, D. Finley, Cell cycle-regulated modification of the ribosome by a variant multiubiquitin chain, Cell 102 (2000) 67–76.
[16] A. Williamson, K.E. Wickliffe, B.G. Mellone, L. Song, G.H. Karpen, M. Rape, Identification of a physiological E2 module for the human anaphase-promoting complex, Proc. Natl. Acad. Sci. U. S. A. 106 (2009) 18213–18218.
[17] P. Xu, D.M. Duong, N.T. Seyfried, D. Cheng, Y. Xie, J. Robert, J. Rush, M. Hochstrasser, D. Finley, J. Peng, Quantitative proteomics reveals the function of unconventional ubiquitin chains in proteasomal degradation, Cell 137 (2009) 133–145.
[18] R. Varadan, M. Assfalg, A. Haririnia, S. Raasi, C. Pickart, D. Fushman, Solution conformation of Lys63-linked di-ubiquitin chain provides clues to functional diversity of polyubiquitin signaling, J. Biol. Chem. 279 (2004) 7055–7063.
[19] R. Varadan, O. Walker, C. Pickart, D. Fushman, Structural properties of polyubiquitin chains in solution, J. Mol. Biol. 324 (2002) 637–647.
[20] M.J. Eddins, R. Varadan, D. Fushman, C.M. Pickart, C. Wolberger, Crystal structure and solution NMR studies of Lys48-linked tetraubiquitin at neutral pH, J. Mol. Biol. 367 (2007) 204–211.
[21] R. Beal, Q. Deveraux, G. Xia, M. Rechsteiner, C. Pickart, Surface hydrophobic residues of multiubiquitin chains essential for proteolytic targeting, Proc. Natl. Acad. Sci. U. S. A. 93 (1996) 861–866.
[22] R.E. Beal, D. Toscano-Cantaffa, P. Young, M. Rechsteiner, C.M. Pickart, The hydrophobic effect contributes to polyubiquitin chain recognition, Biochemistry 37 (1998) 2925–2934.
[23] D. Fushman, K.D. Wilkinson, Structure and recognition of polyubiquitin chains of different lengths and linkage, F1000 Biol. Rep. 3 (2011) 26.
[24] B.C. Dickinson, R. Varadan, D. Fushman, Effects of cyclization on conformational dynamics and binding properties of Lys48-linked di-ubiquitin, Protein Sci. 16 (2007) 369–378.
[25] R. Varadan, M. Assfalg, S. Raasi, C. Pickart, D. Fushman, Structural determinants for selective recognition of a Lys48-linked polyubiquitin chain by a UBA domain, Mol. Cell 18 (2005) 687–698.
[26] J.J. Sims, A. Haririnia, B.C. Dickinson, D. Fushman, R.E. Cohen, Avid interactions underlie the Lys63-linked polyubiquitin binding specificities observed for UBA domains, Nat. Struct. Mol. Biol. 16 (2009) 883–889.
[27] S. Raasi, R. Varadan, D. Fushman, C.M. Pickart, Diverse polyubiquitin interaction properties of ubiquitin-associated domains, Nat. Struct. Mol. Biol. 12 (2005) 708–714.
[28] A. Haririnia, M. D'Onofrio, D. Fushman, Mapping the interactions between Lys48- and Lys63-linked di-ubiquitins and a ubiquitin-interacting motif of S5a, J. Mol. Biol. 368 (2007) 753–766.
[29] D. Zhang, S. Raasi, D. Fushman, Affinity makes the difference: nonselective interaction of the UBA domain of Ubiquilin-1 with monomeric ubiquitin and polyubiquitin chains, J. Mol. Biol. 377 (2008) 162–180.

[30] N. Zhang, Q. Wang, A. Ehlinger, L. Randles, J.W. Lary, Y. Kang, A. Haririnia, A.J. Storaska, J.L. Cole, D. Fushman, K.J. Walters, Structure of the s5a:k48-linked diubiquitin complex and its interactions with rpn13, Mol. Cell 35 (2009) 280–290.
[31] Y. Ryabov, D. Fushman, Interdomain mobility in di-ubiquitin revealed by NMR, Proteins 63 (2006) 787–796.
[32] Y.E. Ryabov, D. Fushman, A model of interdomain mobility in a multidomain protein, J. Am. Chem. Soc. 129 (2007) 3315–3327.
[33] Y.E. Ryabov, D. Fushman, Structural assembly of multidomain proteins and protein complexes guided by the overall rotational diffusion tensor, J. Am. Chem. Soc. 129 (2007) 7894–7902.
[34] W.J. Cook, L.C. Jeffrey, M. Carson, C. Zhijian, C.M. Pickart, Structure of a diubiquitin conjugate and a model for interaction with ubiquitin conjugating enzyme (E2), J. Biol. Chem. 267 (1992) 16467–16471.
[35] A.D.J. van Dijk, D. Fushman, A.M. Bonvin, Various strategies of using residual dipolar couplings in NMR-driven protein docking: application to Lys48-linked di-ubiquitin and validation against ^{15}N-relaxation data, Proteins 60 (2005) 367–381.
[36] J.F. Trempe, N.R. Brown, M.E. Noble, J.A. Endicott, A new crystal form of Lys48-linked diubiquitin, Acta Crystallogr. Sect. F Struct. Biol. Cryst. Commun. 66 (2010) 994–998.
[37] W.J. Cook, L.C. Jeffrey, E. Kasperek, C.M. Pickart, Structure of tetraubiquitin shows how multiubiquitin chains can be formed, J. Mol. Biol. 236 (1994) 601–609.
[38] C.L. Phillips, J. Thrower, C.M. Pickart, C.P. Hill, Structure of a new crystal form of tetraubiquitin, Acta Crystallogr. D Biol. Crystallogr. 57 (2000) 341–344.
[39] M.T. Haldeman, G. Xia, E.M. Kasperek, C.M. Pickart, Structure and function of ubiquitin conjugating enzyme E2-25K: the tail is a core-dependent activity element, Biochemistry 36 (1997) 10526–10537.
[40] F.W. Studier, Protein production by auto-induction in high density shaking cultures, Protein Expr. Purif. 41 (2005) 207–234.
[41] R. Varadan, M. Assfalg, D. Fushman, Using NMR spectroscopy to monitor ubiquitin chain conformation and interactions with ubiquitin-binding domains, in: R.J. Deshaies (Ed.), Ubiquitin and Protein Degradation, Methods in Enzymology, vol. 399 part B, 2005, pp. 177–192.
[42] Z. Otwinowski, W. Minor, Processing of X-ray diffraction data collected in oscillation mode, in: C.W. Carter Jr., R.M. Sweet (Eds.), Macromolecular Crystallography, 1997, pp. 307–326.
[43] A. Vagin, A. Teplyakov, An approach to multi-copy search in molecular replacement, Acta Crystallogr. D Biol. Crystallogr. 56 (2000) 1622–1624.
[44] E. Potterton, P. Briggs, M. Turkenburg, E. Dodson, A graphical user interface to the CCP4 program suite, Acta Crystallogr. D Biol. Crystallogr. 59 (2003) 1131–1137.
[45] A. Vagin, A. Teplyakov, Molecular replacement with MOLREP, Acta Crystallogr. D Biol. Crystallogr. 66 (2010) 22–25.
[46] G.N. Murshudov, A.A. Vagin, E.J. Dodson, Refinement of macromolecular structures by the maximum-likelihood method, Acta Crystallogr. D Biol. Crystallogr. 53 (1997) 240–255.
[47] T. Tenno, K. Fujiwara, H. Tochio, K. Iwai, E.H. Morita, H. Hayashi, S. Murata, H. Hiroaki, M. Sato, K. Tanaka, M. Shirakawa, Structural basis for distinct roles of Lys63- and Lys48-linked polyubiquitin chains, Genes Cells 9 (2004) 865–875.
[48] D. Fushman, R. Varadan, M. Assfalg, O. Walker, Determining domain orientation in macromolecules by using spin-relaxation and residual dipolar coupling measurements, Prog. Nucl. Magn. Reson. Spectrosc. 44 (2004) 189–214.
[49] K.S. Ryu, K.J. Lee, S.H. Bae, B.K. Kim, K.A. Kim, B.S. Choi, Binding surface mapping of intra and inter domain interactions among hHR23B, ubiquitin and poly ubiquitin binding site 2 of S5a, J. Biol. Chem. 278 (2003) 36621–36627.
[50] T.D. Mueller, M. Kamionka, J. Feigon, Specificity of the interaction between ubiquitin-associated domains and ubiquitin, J. Biol. Chem. 279 (2004) 11926–11936.
[51] T. Wang, L. Yin, E.M. Cooper, M.Y. Lai, S. Dickey, C.M. Pickart, D. Fushman, K.D. Wilkinson, R.E. Cohen, C. Wolberger, Evidence for bidentate substrate binding as the basis for the K48 linkage specificity of otubain 1, J. Mol. Biol. 386 (2009) 1011–1023.
[52] J.J. Sims, R.E. Cohen, Linkage-specific avidity defines the lysine 63-linked polyubiquitin-binding preference of rap80, Mol. Cell 33 (2009) 775–783.
[53] M.L. Matsumoto, K.E. Wickliffe, K.C. Dong, C. Yu, I. Bosanac, D. Bustos, L. Phu, D.S. Kirkpatrick, S.G. Hymowitz, M. Rape, R.F. Kelley, V.M. Dixit, K11-linked polyubiquitination in cell cycle control revealed by a K11 linkage-specific antibody, Mol. Cell 39 (2010) 477–484.
[54] E. Krissinel, K. Henrick, Inference of macromolecular assemblies from crystalline state, J. Mol. Biol. 372 (2007) 774–797.
[55] T. Hirano, O. Serve, M. Yagi-Utsumi, E. Takemoto, T. Hiromoto, T. Satoh, T. Mizushima, K. Kato, Conformational dynamics of wild-type Lys48-linked diubiquitin in solution, J. Biol. Chem. 286 (2011) 37486–37502.